November 15, 1994

A Preliminary Optical Visibility Model

K. Cowles
Communications Systems Research Section

B. M. Levine
Optical Sciences and Applications Section

A model is being created to describe the effect of weather on optical communications links between space and ground sites. This article describes the process by which the model is developed and gives preliminary results for two sites. The results indicate nighttime attenuation of optical transmission at five wavelengths. It is representative of a sampling of nights at Table Mountain Observatory from January to June and Mount Lemmon Observatory from May and June. The results are designed to predict attenuation probabilities for optical communications links.

I. Introduction

Space-to-ground visibility statistics are being collected to develop a weather model for optical communications. The Autonomous Visibility Monitoring (AVM) task has deployed two remote observing stations to measure starlight transmission and to calculate attenuation probabilities from which we will create the model. The details of the observing stations have been discussed previously [1]. This article explains the process by which the data are turned into a visibility model for optical communications, and the preliminary data are interpreted. There are two remote observing sites and one test site. The AVM site at the Table Mountain Facility (TMF) has been officially operational since April 1, 1994, while the Mount Lemmon site began operations on May 16, 1994. The test site at the JPL mesa site is not currently operational. Data collected through June 30 are presented here. We will show the theory behind the model, analysis of the initial data, and calibration of those data.

II. Theory

The automated observatories conduct star observations at each site continuously, with pauses for data transfer back to JPL and closures due to weather. The operational station software algorithm directs the system to observe four stars per hour at each of five filters, saving the image and related information in a standard Flexible Image Transport System (FITS) format. Each observation contains information about what is contained in the image as well as conditions at the observatory, such as a weather report and status of the backup power system. The FITS files are compressed and then transferred by modem to JPL for analysis.

The basis of the atmospheric transmission measurement in the AVM system comes from radiation transfer theory, which states that the attenuation of light is logarithmically proportional to the amount of atmosphere it traverses [2]. This relationship is given by the equation

$$I = I_0 10^{-0.4 m_e X} \qquad (1)$$

where

$$I = \text{intensity measured on the ground}$$

$$I_0 = \text{(absolute) intensity of the object above the atmosphere}$$

$$m_e = \text{atmospheric loss factor}$$

$$X = \text{amount of atmosphere traversed}$$

The latter quantity is expressed in units of air mass. One air mass is the amount of atmosphere at zenith, and the amount of atmosphere traversed is roughly proportional to the inverse of the cosine of the zenith pointing angle [3], i.e.,

$$X \sim \frac{1}{\cos \ (\text{zenith angle})} \qquad (2)$$

The atmospheric transmission is given by the ratio of received intensity to that above the atmosphere:

$$\text{transmission} = \frac{I}{I_0} \qquad (3)$$

The transmission is related to the attenuation by the relation,

$$\text{attenuation (dB)} = -10 \ \log_{10} (\text{transmission}) = 4 m_e X \qquad (4)$$

From Eq. (1), there is a log linear relationship between the observed quantities of received intensity and the air mass. The unknowns are the absolute intensity at each wavelength above the atmosphere and the atmospheric loss. The absolute intensity, I_0, is determined through calibration, and will be discussed later. If we assume I_0 is a known quantity, the atmospheric loss can be determined from a given observation.

Automatic algorithms locate the star within the frame of the charge-coupled device (CCD) and integrate the measured values of intensity. In practice, this is determined by summing all intensity values in the frame above a background threshold. All observations are normalized for known star magnitude and observation exposure time.

III. Data Analysis and Model Generation

The atmospheric transmission values over all five filters for each night of observation are saved in summary files along with other observational specific information. The transmission values are normalized by their zenith angle to yield a zenith attenuation according to the equation

$$a_{zen} = -\left(\frac{10}{X}\right) \log \text{transmission (dB)} \qquad (5)$$

The AVM model is defined as a cumulative density function compiled from the ensemble of all zenith attenuation measurements at each filter for each site.

The AVM model based on current data is shown in Figs. 1 and 2. These curves are similar to the telecommunications interfaces for atmospheric and environmental effects data for X-band (8420 MHz), S-band (2295 MHz), and Ka-band (32 GHz).[1] Error bars are drawn corresponding to ± 2 standard deviations of the computed value for each cumulative probability [4].

Figure 1 shows the cumulative attenuation probability for the TMF at each of the five filters. While the TMF AVM telescope did not officially begin observations until April 1, some observations were taken during testing, beginning on January 29. The curves include nighttime observations only and exclude nights when the telescope was down for maintenance. The number of observations included for each curve is indicated.

Cloudy data and clear sky data are incorporated to indicate the probability of link attenuation less than the amounts given on the x-axis. For example, in Fig. 1(b) we see that for the TMF at 532 nm, attenuation was less than 2 dB for 42 percent of the nights and less than 8 dB for 69 percent of the nights during the months of February to June.

Data for Mount Lemmon at each filter is shown in Fig. 2. Comparison of the Mount Lemmon curves with the TMF curves shows that transmission is better at Mount Lemmon. This is expected, since the elevation of Mount Lemmon is 500 m higher than TMF. In Fig. 2(b), attenuation at Mount Lemmon at 532 nm is seen to be less than 2 dB for 62 percent of the nights and less than 8 dB for 73 percent of the nights during May and June.

Looking at the curves for each site, we see that the 532-nm-filter (filter no. 3) data and the V-filter (filter no. 6) data are similar, as are the 860-nm-filter (filter no. 2) and the I-filter (filter no. 4) data. The V, R (filter no. 5), and I filters are astronomical standards and have a much larger bandwidth. However, the V filter is centered near 532 nm and the I is centered near 860 nm, so we expect a similarity in these observations. The initial slope of the 860-nm and I curves is also much steeper than that of the 532-nm and V curves. This is expected because Earth's atmosphere is less transmissive at 532 nm (green) than at 860 nm (near infrared).

Similar curves will be generated for each quarter of the year. The data presented here are slightly misleading because they represent different periods of time. The Mount Lemmon data also have substantially fewer data points and, hence, a larger margin of error.

IV. Analysis and Calibration of I_0

Absolute intensity at each wavelength above the atmosphere can be solved by observing a set of intensity values taken from observations of stars normalized by their magnitudes and zenith pointing angles over a clear sky, and by performing a least-squares fit. From shot-noise considerations, the variations in the received intensity are proportional to the intensity itself, so a weighted least-squares fit is performed. The weighting is determined by the relationship between the intensity and measurements made on the CCD detector.

After the intensity of each observation is determined, a number of procedures examine the night's data for self-consistency and eliminate any outliers from the subsequent calibration routines. These procedures both perform the weighted least-squares fits and examine the resultant spread of the data from the fits.

---

[1] S. C. Slobin, "TCI-40: Telecommunications Interfaces, Atmospherics and Environmental Effects," *Deep Space Network/Flight Project Interface Design Handbook, Volume I: Existing DSN Capabilities*, DSN Document 810-5, Rev. D (internal document), Jet Propulsion Laboratory, Pasadena, California, 1992.
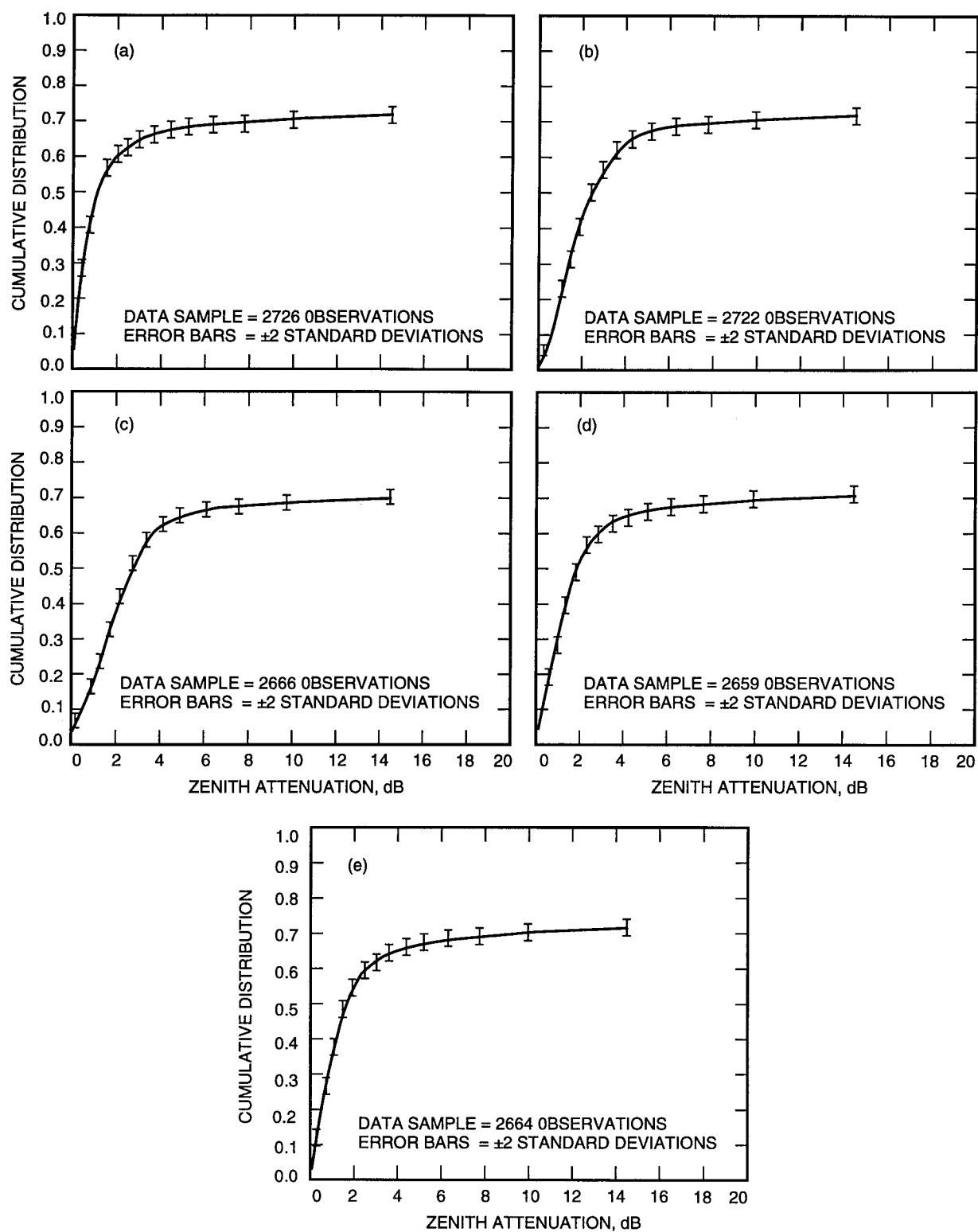
Fig. 1. TMF weather model cumulative attenuation probability from January 29 to June 30, 1994: (a) 860-nm filter; (b) 532-nm filter; (c) V (532-nm) filter; (d) R (680-nm) filter; and (e) I (860-nm) filter.
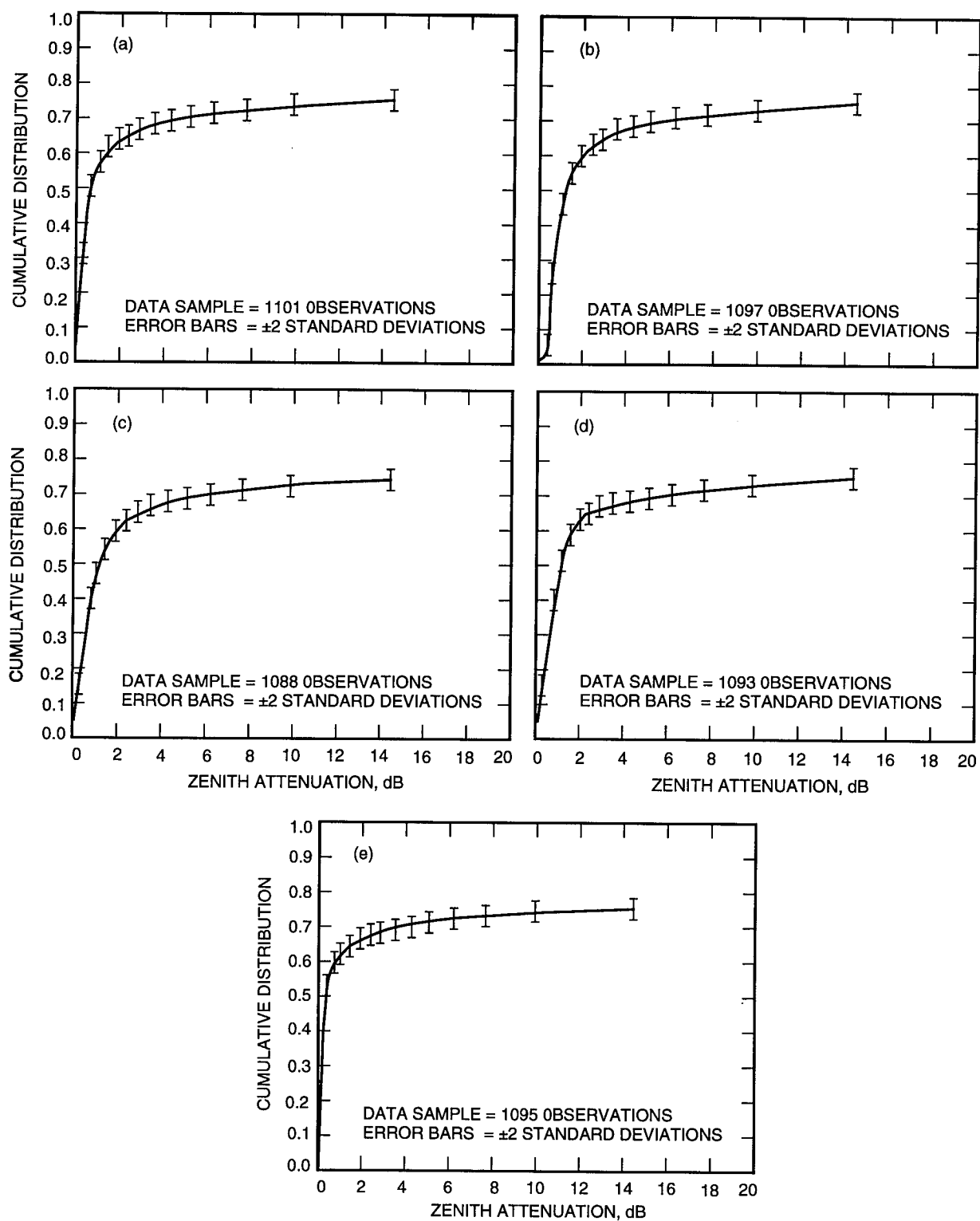
Fig. 2. Mount Lemmon weather model cumulative attenuation probability from May 18 to June 30, 1994: (a) 860-nm filter; (b) 532-nm filter; (c) V (532-nm) filter; (d) R (680-nm) filter; and (e) I (860-nm) filter.
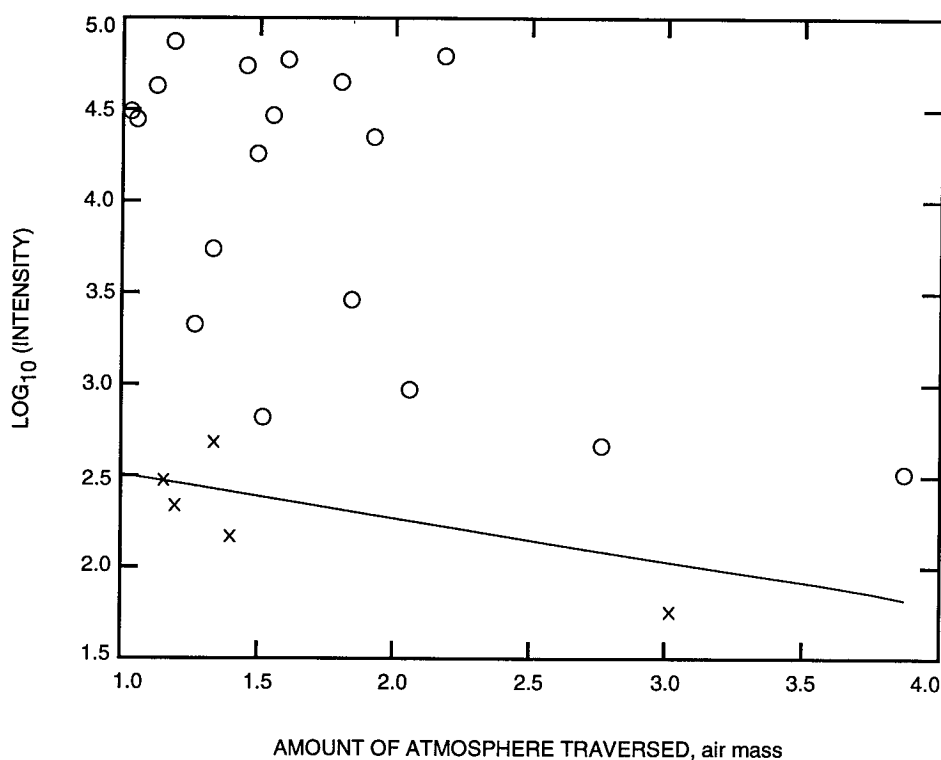
Fig. 3. Least-squares fit with exrtremely low data points.

The first procedure finds those data with intensities representing observations that do not belong to the calibration data set. In Fig. 3, the line drawn on the graph indicates the least-squares fit with the data points marked "X," which are subsequently eliminated. These excluded data values are extremely low, and the resultant least-squares fits would tend to bypass the majority of the data set. Therefore, only the outlier data would be close to these fit, and, hence, should be eliminated before testing the data set for less gross outliers.

The second procedure is based on the "jackknife" statistical technique [5,6] in which one observation is deleted from the data set, and the weighted least-squares solution is determined. This is repeated for every observation, with the result that data that do not belong to the data set will unduly influence the weighed least-squares results and can be identified. If data are deleted, the procedure is repeated on the reduced data set until no further outliers are detected. One iteration of this process is shown in Fig. 4; the data point marked "X" has been identified as an outlier. The two lines on the graph indicate the least-squares fit with and without the data point at 6 air masses.

After all outliers have been removed, the atmospheric loss is calculated for the night. Figure 5 shows the final fit for the data taken the night of June 7–8 at Mount Lemmon. Extrapolating the line to zero air mass, we determine the best estimate of the absolute intensity for that night at the 532-nm filter.

Transmission is computed by the quotient of the measured intensity of a set of observations divided by the best estimate of the absolute intensity. This estimate is formed from all estimates of absolute intensity that are self-consistent. Consistency is tested by comparing the current measurement of I_0 with an updated value of I_0 using historical plus current data. If the data set under examination produces a consistent value of I_0, then it is incorporated into the best estimate. This test is performed for every data set taken. The results from one night's observations at Mount Lemmon are shown in Table 1.
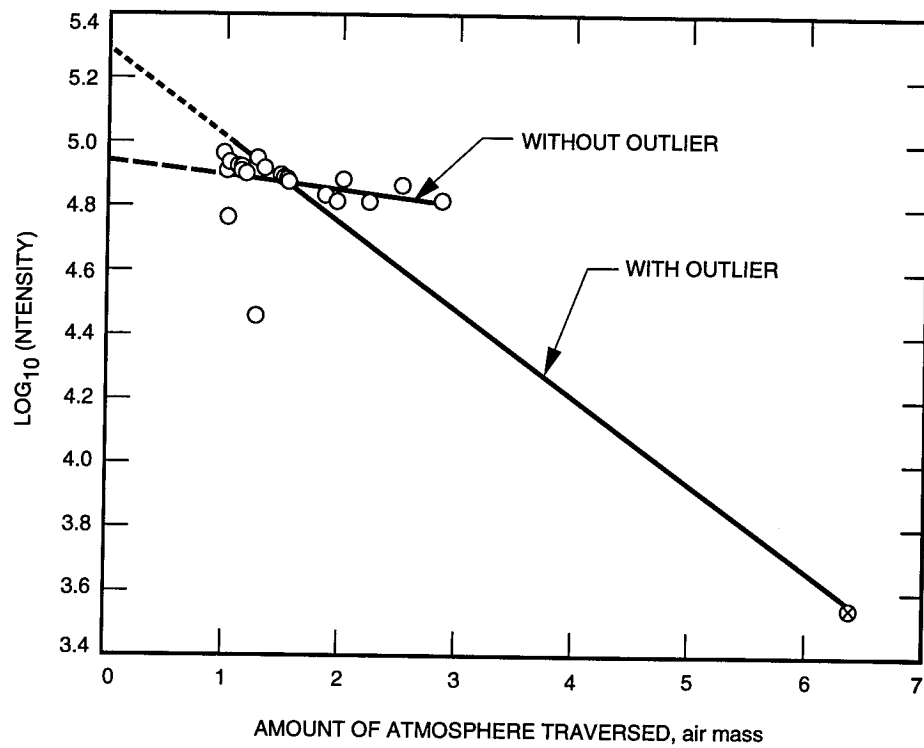
Fig. 4

LOG$_{10}$ (INTENSITY)

WITHOUT OUTLIER

WITH OUTLIER

AMOUNT OF ATMOSPHERE TRAVERSED, air mass

Fig. 4. Outlier removal using the jackknife statistical technique.

Fig. 5

LOG$_{10}$ (INTENSITY)

DATA SIZE = 25 of 33 samples
I_0 = 90889.0 DN
M_e = 0.1748 magnitude/air mass
RMS DIFFERENCE = 3.80 percent

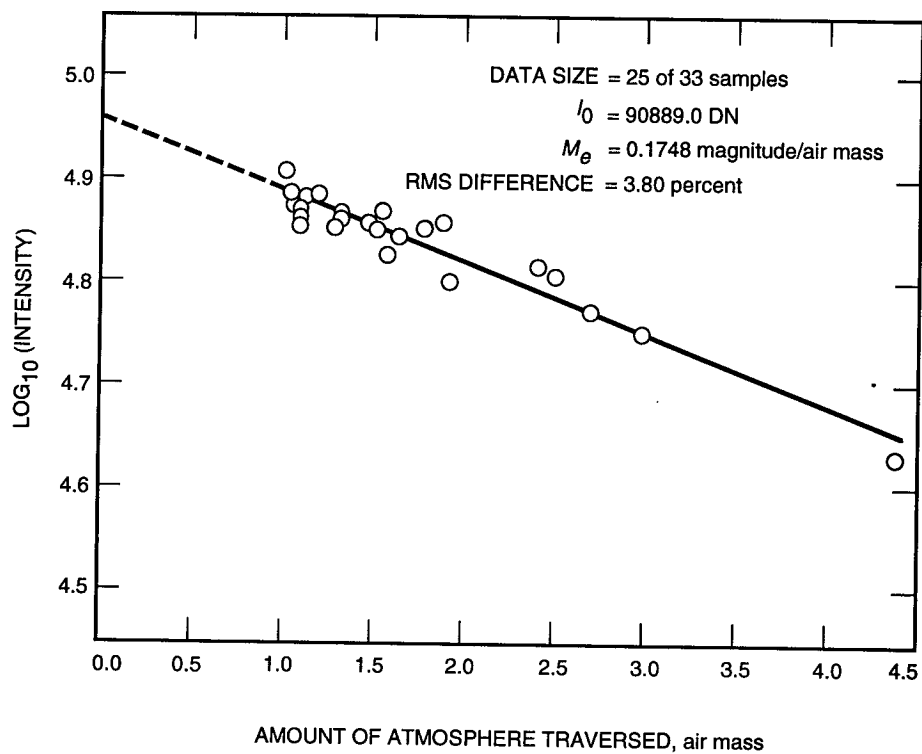AMOUNT OF ATMOSPHERE TRAVERSED, air mass

Fig. 5. Best fit of data points to determine I_0.

For each filter, the calculated values of I_0 and m_e are given along with the relative rms error expressed in percent and the average transmission of the sky. The remainder of the columns show the results of eliminating data from the final calibration set. Starting with the total number of files, the data eliminated from the two procedures mentioned above are given in the #Xs and #tol columns, respectively. The #misc and #Os columns denote those values eliminated due to pointing at zenith angles greater than 85 deg and those data in which an intensity above background could not be detected, respectively.

Table 2 shows the old and updated values of I_0 along with the f-statistic and the degrees of freedom. The f-statistic algorithm is a test for consistency for the new and old I_0. If the data are consistent with previous measurements, the data values for the night are included in the calibration of I_0 for that filter. Confidence in I_0 will increase as the number of observations included in the calibration increases. The I_0's are then used to calculate the atmospheric loss for the night.

Table 1. Daily report for Mount Lemmon on the night of June 7–8, 1994.

Filter no.	I_0	m_e	Relative rms error, percent	Average transmission of the sky	#files	#misc	#0s	#Xs	#tol	#left[a]
6	841597	0.1201	8.8639	0.8953	33	1	1	1	5	25
5	649404	0.1142	3.9662	0.9002	33	0	2	3	8	20
4	370191	0.0630	10.4121	0.9437	33	0	1	1	4	27
3	90889	0.1748	3.7965	0.8513	33	0	2	4	2	25
2	25956	0.0522	10.2851	0.9530	33	1	1	1	3	27

[a] #left = #files −(#misc. + #0s + #Xs + #tol).

Table 2. IO calibration for Mount Lemmon.

Filter no.	Cumulative I_0 (old)	Cumulative I_0 (new)	f-statistic	Degrees of freedom
6	768396	782163	1.7012	175
5	638065	639062	0.1011	162
4	210833	228700	0.2064	209
3	88646	89070	0.5346	163
2	28148	27672	3.2679	170

V. Performance

The AVM observatory at TMF has been operating officially since April 1, 1994. However, data taken between April 27 and June 22 have been removed from the database because, due to system malfunction, they were not representative of the site. As a result, the data are those for 40 percent of the period between January 29 and April 1, 1994, and for 32 percent of the period between April 1 and June 30, 1994. The system has been repaired and is now functioning routinely.

The AVM site at Mount Lemmon was operational 79 percent of the period between May 18 and June 30, 1994. Downtime outages at both sites occurred because of temporary system malfunction or maintenance periods.

VI. Conclusions

Preliminary data from the AVM sites at TMF and Mount Lemmon have provided data adequate to prepare preliminary cumulative distribution curves for the wavelengths measured. These curves can be used to predict link availability for the sites. A set of curves such as these will be produced each quarter to show variation in site characteristics by season. The data can be analyzed for all or part of a year as required.

Further studies include calculation of joint statistics for the two sites, as well as incorporation of daytime transmission data. The data can also be compared with satellite weather data to define the correlation between the two methods of clear-sky detection. Several scenarios can then be studied for a spacecraft-to-ground optical communications link.

References

[1] K. Cowles, "Hardware Design for the Autonomous Visibility Monitoring Observatory," *The Telecommunications and Data Acquisition Progress Report 42-114, vol. April–June 1993*, Jet Propulsion Laboratory, Pasadena, California, pp. 295–301, August 15, 1993.

[2] W. A. Hiltner, ed., *Astronomical Techniques*, vol. 2 of Star and Stellar Systems, Chicago: University of Chicago Press, p. 179, 1960.

[3] C. W. Allen, *Astrophysical Qualities*, London: Athens Press, Section 55, pp. 124–125, 1976.

[4] A. M. Mood, F. A. Graybill, and D. C. Boes, *Introduction to the Theory of Statistics*, 3rd ed., New York: McGraw-Hill Book Company, Chapter 11, Section 2.1, 1974.

[5] B. Efron, *The Jackknife, the Bootstrap and other Resampling Plans*, Conference Board of Mathematical Science-NSF Regional Conference Series in Applied Mathematics, 1982.

[6] C. Z. Mooney and R. D. Duval, *Bootstrapping: A Nonparametric Approach to Statistical Inference*, Newbury Park: SAGE Publications, p. 22, 1993.